Global-Local Regularization Via Distributional Robustness

Hoang Phan$^\diamond$ Trung Le† Trung Phung$^\diamond$ Tuan Anh Bui† Nhat Ho‡ Dinh Phung†

Monash University, Australia †; VinAI Research$^\diamond$; University of Texas, Austin‡
March 1, 2022

Abstract

Despite superior performance in many situations, deep neural networks are often vulnerable to adversarial examples and distribution shifts, limiting model generalization ability in real-world applications. To alleviate these problems, recent approaches leverage distributional robustness optimization (DRO) to find the most challenging distribution, and then minimize loss function over this most challenging distribution. Regardless of achieving some improvements, these DRO approaches have some obvious limitations. First, they purely focus on local regularization to strengthen model robustness, missing a global regularization effect which is useful in many real-world applications (e.g., domain adaptation, domain generalization, and adversarial machine learning). Second, the loss functions in the existing DRO approaches operate in only the most challenging distribution, hence decouple with the original distribution, leading to a restrictive modeling capability. In this paper, we propose a novel regularization technique, following the veins of Wasserstein-based DRO framework. Specifically, we define a particular joint distribution and Wasserstein-based uncertainty, allowing us to couple the original and most challenging distributions for enhancing modeling capability and applying both local and global regularizations. Empirical studies on different learning problems demonstrate that our proposed approach significantly outperforms the existing regularization approaches in various domains: semi-supervised learning, domain adaptation, domain generalization, and adversarial machine learning.

1 Introduction

Despite achieving state-of-the-art performance in many real-world applications, deep neural networks are often vulnerable to adversarial examples and distribution shifts, limiting model generalization ability in real-world applications. To relieve these issues, in addition to some regularization techniques, e.g., VAT [49], ADT [13], ME-ADA [75], Mixup [72], Cutout [12] and Cutmix [70], distributional robustness (DR) is an emerging framework for improving model robustness and regularization ability, which seeks the worst-case expected loss among a ball of distributions, containing all distributions that are close to the empirical distribution [18].

As the Wasserstein distance is a powerful and convenient tool of measuring closeness between distributions, Wasserstein DR has been one of the most widely-used variant of DR. Here we consider a generic Polish space S endowed with a distribution $\mathbb{P}$. Let $r : S \to \mathbb{R}$ be a real-valued (risk) function and $c : S \times S \to \mathbb{R}_+$ be a cost function. Distributional robustness setting aims to find the distribution $\tilde{\mathbb{P}}$ in the vicinity of $\mathbb{P}$ and maximizes the risk in the $\mathbb{E}$ form [61, 4]:

$$\sup_{\tilde{\mathbb{P}}:\mathcal{W}_c\left(\mathbb{P},\tilde{\mathbb{P}}\right)<\epsilon} \mathbb{E}_{\tilde{Z}\sim\tilde{\mathbb{P}}}\left[r\left(\tilde{Z}\right)\right], \tag{1}$$

where $\epsilon > 0$ and $\mathcal{W}_c$ denotes the optimal transport (OT) cost or a Wasserstein (WS) distance if c is a metric, defined

$$\mathcal{W}_c\left(\mathbb{P},\tilde{\mathbb{P}}\right) := \inf_{\gamma\in\Gamma\left(\mathbb{P},\tilde{\mathbb{P}}\right)} \int cd\gamma, \tag{2}$$

where $\Gamma\left(\mathbb{P},\tilde{\mathbb{P}}\right)$ is the set of couplings whose marginals are $\mathbb{P}$ and $\tilde{\mathbb{P}}$. With the assumption that $r \in L^1\left(\mathbb{P}\right)$ is upper semi-continuous and the cost c is a non-negative lower semi-continuous satisfying $c(Z,\tilde{Z}) = 0$ iff $Z = \tilde{Z}$, [61, 4] show that the *dual* form for equation (1) is:

$$\inf_{\lambda\geq 0}\left\{\lambda\epsilon + \mathbb{E}_{Z\sim\mathbb{P}}\left[\sup_{\tilde{Z}}\left\{r\left(\tilde{Z}\right) - \lambda c\left(\tilde{Z},Z\right)\right\}\right]\right\}. \tag{3}$$

When applying DR to the classification problem, $\tilde{Z} = \left(\tilde{X},\tilde{Y}\right)$ is a pair of data/label drawn from $\tilde{\mathbb{P}}$ and r is the loss function [61, 4]. Obviously, the fact that r involves only $\tilde{Z} = \left(\tilde{X},\tilde{Y}\right) \sim \tilde{\mathbb{P}}$ certainly restricts the modeling capacity of (1). Specifically, in the primal form equation (1), we find the *most challenging distribution* $\tilde{\mathbb{P}}$, while in the dual form (3), we find the *most challenging sample* $\tilde{Z}$ around $Z \sim \mathbb{P}$ by maximizing $r\left(\tilde{Z}\right)$. However, because r involves only $\tilde{Z}$ in its formulation, it is *impossible* to find the most challenging sample if it requires to compare the prediction probabilities for Z and $\tilde{Z}$ (e.g., Kullback-Leibler (KL) divergence $KL\left(p\left(\tilde{Z}\right)\|p(Z)\right)$ as in TRADES [74]). Moreover, it is also *impossible* to inject a *global regularization term* requiring the involvement of a batch of samples $\tilde{Z}$ and Z.

To empower the formulation of DR for efficiently and effectively tackling various real-world applications, in this work, we propose a rich OT based DR framework, named **G***lobal*-**L***ocal* **O***ptimal* **T***ransport based* **D***istributional* **R***obustness* (GLOT-DR). Specifically, by designing special joint distributions $\mathbb{P}$ and $\tilde{\mathbb{P}}$ together with some constraints, our framework is applicable to a mixed variety of real-world applications, including *domain generalization* (DG), *domain adaptation* (DA), *semi-supervised learning* (SSL), and *adversarial machine learning* (AML). Additionally, our GLOT-DR makes us possible to equip a *local regularization term* for enforcing a local smoothness and robustness and a *global regularization term* for enforcing a global effect targeting a downstream task. Moreover, by designing a specific WS distance, we successfully develop a closed-form solution for GLOT-DR without using the dual form in [61, 4] (i.e., equation (3)). Technically, our solution turns solving the inner maximization in the dual form (3) to sampling a set of challenging particles according to a local distribution on which we can handle efficiently using Stein Variational Gradient Decent (SVGD) [39]. Based on the general framework of GLOT-DR, we establish the settings for DG, DA, SSL, and AML and conduct experiments to compare our GLOT-DR to state-of-the-art baselines in these real-world applications. Overall, our contributions can be summarized as follows:

1. We enrich the general framework of DR to make it possible for many real-world applications including DG, DA, SSL, and AML by enforcing both local and global regularization terms. Here we note that the global regularization term is crucial for a downstream task, e.g.,

bridging the distribution shift between source and target domains in DA, between labeled and unlabeled portions in SSL, and benign and adversarial data examples in AML, and learning domain invariant features in DG.

2. We propose a closed-form solution for our GLOT-DR without involving the dual form in [61, 4] (i.e., equation (3)). Here we note that the dual form (3) is *not computationally convenient* to solve due to the minimization over λ.

3. We conduct comprehensive experiments to compare our GLOT-DR to state-of-the-art baselines in DG, DA, SSL, and AML accordingly. The experimental results demonstrate the merits of our proposed approach.

2 Related Work

Distributional robustness (DR). DR is a promising framework to enhance model robustness. The underlying idea of DR is to find the *most challenging distribution* around a given distribution and then challenge a model with this distribution. To characterize the closeness of a distribution to a center distribution, either a f-divergence [2, 50, 53, 15, 14] or Wasserstein distance [51, 60, 19, 28, 3] can be employed. Other works [61, 4] developed a dual form for DR, opening a door to incorporate DR into the training process of deep learning models.

Adversarial Robustness (AR). Neural networks are generally vulnerable to adversarial attacks, notably FGSM [21], PGD [46], and Auto-Attack [8]. Among various kinds of defense approaches, Adversarial Training (AT), originating in [21], has drawn the most research attention. Given its effectiveness and efficiency, many variants of AT have been proposed with (1) different types of adversarial examples (e.g., the worst-case examples [21] or most divergent examples [74]), (2) different searching strategies (e.g., non-iterative FGSM and Rand FGSM [46]), (3) additional regularization (e.g., adding constraints in the latent space [73, 7]). DR has been applied to improve model robustness in [61, 63, 49, 52, 31, 13].

Transfer Learning (TL). Domain adaptation (DA) and domain generalization (DG) are two typical settings in TL. Specifically, the works in DA [17, 41, 10, 35] aim at training a model based on a labeled source domain to adapt to an unlabeled target domain, while the works in DG [5, 32, 33, 47, 1, 34] aim at training a model based on multiple labeled source domains to predict well on unseen target domains. DR was leveraged with DG in [75] and DA in [68].

3 Proposed Approach

In this section, we first introduce the GLOT-DR framework and provide the theoretical guarantees in Section 3.1. Then Section 3.2 presents the general training procedure of our proposed approach, the detailed formulations of scenarios are described in the remainder of this section.

3.1 Our Framework

We propose a regularization technique based on optimal transport DR, widely applied to many settings including i) *semi-supervised learning* (SSL), ii) *domain adaptation* (DA), iii) *domain generalization* (DG), and iv) *adversarial machine learning* (AML). In what follows, we present the general setting and technical details of our framework.
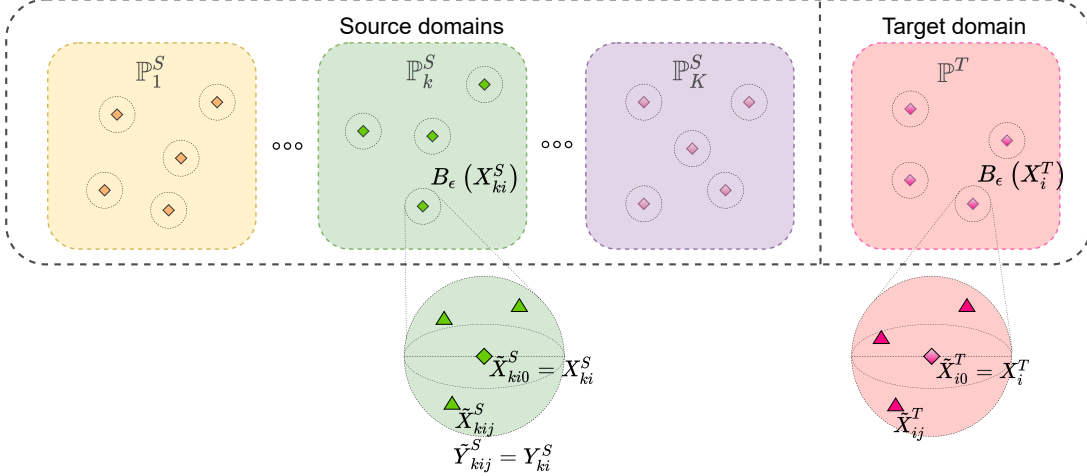
Figure 1: Overview of GLOT-DR. We sample $\left[X_{ki}^S, Y_{ki}^S\right]_{i=1}^{B_k^S}$ for each source domain, $\left[X_i^T\right]_{i=1}^{B^T}$ for the target domain, and define Z as in equation (4). Let $\mathbb{P}$ be the distribution of Z. For $\left(Z, \tilde{Z}\right) \sim \gamma$ satisfying $\mathbb{E}_\gamma\left[\rho\left(Z, \tilde{Z}\right)\right]^{1/q} \leq \epsilon$, we have $\tilde{X}_{ki0}^S = X_{ki0}^S = X_{ki}^S$, $\tilde{X}_{i0}^T = X_{i0}^T = X_i^T$. Besides, $\tilde{X}_{kij}^S$ with $j \geq 1$ can be viewed as the *most challenging* examples in the ball $B_\epsilon\left(X_{ki}^S\right)$, which have the same label Y_{ki}^S. Similarly, $\tilde{X}_{ij}^T$ with $j \geq 1$ can be viewed as the *most challenging* examples in the ball $B_\epsilon\left(X_i^T\right)$.

Assume that we have *multiple labeled source domains* with the *data/label* distributions $\left\{\mathbb{P}_k^S\right\}_{k=1}^K$ and a *single unlabeled target domain* with the *data* distribution $\mathbb{P}^T$. For the k-th source domain, we sample a batch of B_k^S examples as $\left(X_{ki}^S, Y_{ki}^S\right) \overset{\text{iid}}{\sim} \mathbb{P}_k^S$, where $i = 1, \ldots, B_k^S$ is the sample index. Meanwhile, for the target domain, we sample a batch of B^T examples as $X_i^T \overset{\text{iid}}{\sim} \mathbb{P}^T$, $i = 1, \ldots, B^T$. It is worth noting that for the DG setting, we set $B^T = 0$ (i.e., not use any target data in training). Furthermore, we examine the multi-class classification problem with the label set $\mathcal{Y} := \{1, ..., M\}$. Hence, the prediction of a classifier is a prediction probability belonging to the *label simplex* $\Delta_M := \left\{\pi \in \mathbb{R}^M : \|\pi\|_1 = 1 \text{ and } \pi \geq \mathbf{0}\right\}$. Finally, let $f_\psi = h_\theta \circ g_\phi$ with $\psi = (\phi, \theta)$ be parameters of our deep net, wherein g_ϕ is the feature extractor and h_θ is the classifier on top of feature representations.

As explained below, our method involves the construction of a random variable Z with distribution $\mathbb{P}$ and another random variable $\tilde{Z}$ with distribution $\tilde{\mathbb{P}}$, "containing" anchor samples $\left(X_{ki}^S, Y_{ki}^S\right), X_i^T$ and their perturbed counterparts $\left(\tilde{X}_{kij}^S, \tilde{Y}_{kij}^S\right), \tilde{X}_{ij}^T$. The inclusion of both anchor samples and perturbed samples allows us to define a unifying cost function containing local regularization, global regularization and classification loss.

Concretely, we first start with the construction of Z, containing repeated anchor samples

$$Z := \left[\left[\left[X_{kij}^S, Y_{kij}^S\right]_{k=1}^K\right]_{i=1}^{B_k^S}\right]_{j=0}^{n^S}, \left[\left[X_{ij}^T\right]_{i=1}^{B^T}\right]_{j=0}^{n^T}. \tag{4}$$

Here, each source sample is repeated $n^S + 1$ times $\left(X_{kij}^S, Y_{kij}^S\right) = \left(X_{ki}^S, Y_{ki}^S\right)$, $\forall j$, while each target sample is repeated $n^T + 1$ times $X_{ij}^T = X_i^T$, $\forall j$. The corresponding distribution of this random variable is denoted as $\mathbb{P}$. In contrast to Z, we next define random variable $\tilde{Z} \sim \tilde{\mathbb{P}}$, whose form is:

$$\tilde{Z} := \left[\left[\left[\tilde{X}_{kij}^S, \tilde{Y}_{kij}^S\right]_{k=1}^K\right]_{i=1}^{B_k^S}\right]_{j=0}^{n^S}, \left[\left[\tilde{X}_{ij}^T\right]_{i=1}^{B^T}\right]_{j=0}^{n^T}. \tag{5}$$

We would like $\tilde{Z}$ to contain both: i) anchor examples, e.g., $\left(\tilde{X}_{ki0}^S, \tilde{Y}_{ki0}^S\right) = \left(X_{ki}^S, Y_{ki}^S\right)$ and $\tilde{X}_{i0}^T = X_i^T$; ii) n^S perturbed source samples $\left\{\tilde{X}_{kij}^S, \tilde{Y}_{kij}^S\right\}_{j=1}^{n^S}$ and n^T perturbed target samples $\left\{\tilde{X}_{ij}^T\right\}_{i=1}^{n^T}$. In order to enforce this requirements, we only consider sampling $\tilde{Z}$ from distribution $\tilde{\mathbb{P}}$ inside the Wasserstein-ball of $\mathbb{P}$, i.e., satisfying $\mathcal{W}_\rho\left(\mathbb{P}, \tilde{\mathbb{P}}\right) := \inf_{\gamma \in \Gamma(\mathbb{P}, \tilde{\mathbb{P}})} \mathbb{E}_{(Z, \tilde{Z}) \sim \gamma}\left[\rho\left(Z, \tilde{Z}\right)\right]^{\frac{1}{q}} \leq \epsilon$, where the cost metric is defined as

$$\begin{aligned}
\rho\left(Z, \tilde{Z}\right) := &\ \infty \sum_{k=1}^K \sum_{i=1}^{B_k^S} \left\|X_{ki0}^S - \tilde{X}_{ki0}^S\right\|_p^q \\
&+ \infty \sum_{i=1}^{B^T} \left\|X_{i0}^T - \tilde{X}_{i0}^T\right\|_p^q + \sum_{k=1}^K \sum_{i=1}^{B_k^S} \sum_{j=1}^{n^S} \left\|X_{kij}^S - \tilde{X}_{kij}^S\right\|_p^q \\
&+ \sum_{i=1}^{B^T} \sum_{j=1}^{n^T} \left\|X_{ij}^T - \tilde{X}_{ij}^T\right\|_p^q + \infty \sum_{k=1}^K \sum_{i=1}^{B_k^S} \sum_{j=0}^{n^S} \rho_l\left(Y_{kij}^S, \tilde{Y}_{kij}^S\right),
\end{aligned}$$

where ρ_l is a metric on the *label simplex* Δ_M. Here we slightly abuse the notion by using $Y \in \mathcal{Y}$ to represent its corresponding one-hot vector. By definition, this cost metric almost surely : i) enforces all $j = 0$ samples in $\tilde{Z}$ to be anchor samples; ii) allows perturbations on the input data, e.g., $\tilde{X}_{kij}^S \neq X_{ki}^S$ and $\tilde{X}_{ij}^T \neq X_i^T$, for $\forall j \neq 0$; iii) restricts perturbations on labels, e.g., $Y_{kij}^S = \tilde{Y}_{kij}^S$ for $\forall j$ (cf. Figure 1).

Upon clear definitions of $\tilde{Z}$ and $\tilde{\mathbb{P}}$, we wish to learn good representations and regularize the classifier f_ψ, via the following distributional robustness problem:

$$\min_{\theta, \phi} \max_{\tilde{\mathbb{P}} : \mathcal{W}_\rho(\mathbb{P}, \tilde{\mathbb{P}}) \leq \epsilon} \mathbb{E}_{\tilde{Z} \sim \tilde{\mathbb{P}}}\left[r\left(\tilde{Z}; \phi, \theta\right)\right]. \tag{6}$$

The cost function $r\left(\tilde{Z}; \phi, \theta\right) := \alpha r^l\left(\tilde{Z}; \phi, \theta\right) + \beta r^g\left(\tilde{Z}; \phi, \theta\right) + \mathcal{L}\left(\tilde{Z}; \phi, \theta\right)$ with $\alpha, \beta > 0$ is defined as the sum of a *local-regularization function* $r^l\left(\tilde{Z}; \phi, \theta\right)$, a *global-regularization function* $r^g\left(\tilde{Z}; \phi, \theta\right)$, and the *loss function* $\mathcal{L}\left(\tilde{Z}; \phi, \theta\right)$, whose explicit forms are dependent on the task (DA, SSL, DG, AML, etc). Intuitively, the optimization in equation (6) iteratively searches for the worst-case $\tilde{\mathbb{P}}$ w.r.t. the cost $r\left(\cdot; \phi, \theta\right)$, then changes the network f_ψ to minimize the worst-case cost.

Let us define

$$\Gamma_\epsilon := \left\{ \gamma : \gamma \in \cup_{\tilde{\mathbb{P}}} \Gamma\left(\mathbb{P}, \tilde{\mathbb{P}}\right) \text{ and } \mathbb{E}_{(Z,\tilde{Z})\sim\gamma}\left[\rho\left(Z, \tilde{Z}\right)\right]^{1/q} \leq \epsilon \right\},$$

and show that the inner max problem in equation (6) is equivalent to search in Γ_ϵ.

Lemma 1. *(Proof in Appendix A) The optimization problem in equation (6) is equivalent to the following optimization problem:*

$$\min_{\theta,\phi} \max_{\gamma:\in\Gamma_\epsilon} \mathbb{E}_{(Z,\tilde{Z})\sim\gamma}\left[r\left(\tilde{Z}; \phi, \theta\right)\right]. \tag{7}$$

To tackle the optimization problem (OP) in equation (7), we add the entropic regularization and arrive at the following OP:

$$\min_{\theta,\phi} \max_{\gamma:\in\Gamma_\epsilon} \left\{ \mathbb{E}_{(Z,\tilde{Z})\sim\gamma}\left[r\left(\tilde{Z}; \phi, \theta\right)\right] + \frac{1}{\lambda}\mathbb{H}\left(\gamma\right) \right\}, \tag{8}$$

where $\lambda > 0$ is the entropic regularization parameter and $\mathbb{H}$ returns the entropy of a given distribution.

The following theorem indicates the optimal solution of the inner max in the OP in equation (8).

Theorem 2. *(Proof in Appendix A) Assuming $r\left(\tilde{Z}; \psi\right) = \alpha r^l\left(\tilde{Z}; \psi\right) + \beta r^g\left(\tilde{Z}; \psi\right) + \mathcal{L}\left(\tilde{Z}; \psi\right)$ with $\psi = (\phi, \theta)$. In addition, Z and $\tilde{Z}$ are constructed as in equation (4) and equation (5), respectively. Let ℓ denote the loss function, so the expected classification loss becomes*

$$\mathcal{L}\left(\tilde{Z}; \psi\right) := \sum_{k=1}^{K} \sum_{i=1}^{B_k^S} \sum_{j=0}^{n_k^S} \ell\left(\tilde{X}_{kij}^S, \tilde{Y}_{kij}^S; \psi\right).$$

Moreover, let the global-regulazation $r^g\left(\tilde{Z}; \psi\right) := r^g\left(\left[\tilde{X}_{ki0}^S\right]_{k,i}, \left[\tilde{X}_{i0}^T\right]_i; \psi\right)$ depend only on anchor samples, while the local-regularization depend on the differences between anchor samples and perturbed samples,

$$r^l\left(\tilde{Z}; \psi\right) := \sum_{i=1}^{B^T} \sum_{j=1}^{n^T} s\left(\tilde{X}_{i0}^T, \tilde{X}_{ij}^T; \psi\right) + \sum_{k=1}^{K} \sum_{i=1}^{B_k^S} \sum_{j=1}^{n_k^S} s\left(\tilde{X}_{ki0}^S, \tilde{X}_{kij}^S; \psi\right),$$

where $s\left(\tilde{X}_0, \tilde{X}_j; \psi\right)$ measures the difference between 2 input samples, and $s(X, X; \psi) = 0, \forall X$. To this end, the inner max in the OP when $q = \infty$ has the following solution

$$\gamma^*\left(Z, \tilde{Z}\right) = \prod_{k=1}^{K} \prod_{i=1}^{B_k^S} \prod_{j=0}^{n_k^S} p_k^S\left(X_{ki}^S, Y_{ki}^S\right) \prod_{i=1}^{B^T} \prod_{j=0}^{n^T} p^T\left(X_i^T\right)$$

$$\times \prod_{k=1}^{K} \prod_{i=1}^{B_k^S} \prod_{j=0}^{n_k^S} \frac{\exp\left\{\lambda[\alpha s(X_{ki}^S, \tilde{X}_{kij}^S; \psi) + \ell(\tilde{X}_{kij}^S, Y_{ki}^S; \psi)]\right\}}{\int_{B_\epsilon\left(X_{ki}^S\right)} \exp\left\{\lambda[\alpha s(X_{ki}^S, \tilde{X}_{kij}^S; \psi) + \ell(\tilde{X}_{kij}^S, Y_{ki}^S; \psi)]\right\} d\tilde{X}_{kij}^S}$$

$$\times \prod_{i=1}^{B^T} \prod_{j=1}^{n^T} \frac{\exp\left\{\lambda\alpha s\left(X_i^T, \tilde{X}_{ij}^T; \psi\right)\right\}}{\int_{B_\epsilon\left(X_i^T\right)} \exp\left\{\lambda\alpha s\left(X_i^T, \tilde{X}_{ij}^T; \psi\right)\right\}}, \tag{9}$$

6

where $\left(X_{ki}^S, Y_{ki}^S\right)_{i=1}^{B_k^S} \overset{iid}{\sim} \mathbb{P}_k^S, \forall k, X_{1:B^T}^T \overset{iid}{\sim} \mathbb{P}^T, p_k^S$ is the density function of $\mathbb{P}_k^S$, p^T is the density function of $\mathbb{P}^{\mathbb{T}}$, and $B_\epsilon(X) := \left\{ X' : \|X' - X\|_p \leq \epsilon \right\}$.

By substituting the optimal solution in equation (9) back to equation (7), we reach the following OP with $\psi = (\phi, \theta)$:

$$\min_\psi \mathbb{E}_{\forall k: \left(X_{ki}^S, Y_{ki}^S\right)_{i=1}^{B_k^S} \overset{iid}{\sim} \mathbb{P}_k^S, X_{1:B^T}^T \overset{iid}{\sim} \mathbb{P}^T} \left[r\left(\tilde{Z}; \psi\right) \right], \tag{10}$$

where $r\left(\tilde{Z}; \psi\right)$ is defined as

$$\mathbb{E}_{\left[\tilde{X}_{kij}^S\right]_j \sim \mathbb{P}_{ki}^S} \left[\alpha s(X_{ki}^S, \tilde{X}_{kij}^S; \psi) + \ell(\tilde{X}_{kij}^S, Y_{ki}^S; \psi) \right] +$$
$$\mathbb{E}_{\left[\tilde{X}_{ij}^T\right]_j \sim \mathbb{P}_i^T} \left[\alpha s\left(X_i^T, \tilde{X}_{ij}^T; \psi\right) \right] + \beta r^g \left(\left[X_{ki}^S\right]_{k,i}, \left[X_i^T\right]_i; \psi \right), \tag{11}$$

where the *local distribution* $\mathbb{P}_{ki}^S$ over $B_\epsilon\left(X_{ki}^S\right)$ has the density proportional to $\exp\left\{\lambda[\alpha s(X_{ki}^S, \cdot; \psi)\ell(\cdot, Y_{ki}^S; \psi)]\right\}$, and the *local distribution* $\mathbb{P}_i^T$ over $B_\epsilon\left(X_i^T\right)$ has the density proportional to $\exp\left\{\lambda\alpha s\left(X_i^T, \cdot; \psi\right)\right\}$.

It is worth noting the how flexible the global-regularization function $r^g \left(\left[X_{ki}^S\right]_{k,i}, \left[X_i^T\right]_i; \psi \right)$ is in enforcing various characteristics suitable for the task, e.g., bridging the gap between labeled (source) and unlabeled (target) data in SSL and DA, or learning domain-invariant features in DG. Moreover, our global and local regularization terms can be naturally applied to the latent space induced by the feature extractor g_ϕ. Additionally, the theory development for this case is similar to that for the data space except replacing X in the data space by $g_\phi(X)$ in the latent space.

3.2 Training Procedure of Our Approach

In what follows, we present how to solve the OP in equation (10) efficiently. Accordingly, we first need to sample $\left(X_{ki}^S, Y_{ki}^S\right)_{i=1}^{B_k^S} \overset{iid}{\sim} \mathbb{P}_k^S, \forall k$ and $X_{1:B^T}^T \overset{iid}{\sim} \mathbb{P}^T$. For each source anchor $\left(X_{ki}^S, Y_{ki}^S\right)$, we sample $\left[\tilde{X}_{kij}^S\right]_{j=1}^{n^S} \overset{iid}{\sim} \mathbb{P}_{ki}^S$ in the ball $B_\epsilon\left(X_{ki}^S\right)$ with the *density function proportional* to $\exp\left\{\lambda[\alpha s(X_{ki}^S, \bullet; \psi) + \ell(\cdot, Y_{ki}^S; \psi)]\right\}$. Furthermore, for each target anchor X_i^T, we sample $\left[\tilde{X}_{ij}^T\right]_{j=1}^{n^T} \overset{iid}{\sim} \mathbb{P}_i^T$ in the ball $B_\epsilon\left(X_i^T\right)$ with the d*ensity function proportional* to $\exp\left\{\lambda\alpha s\left(X_i^T, \bullet; \psi\right)\right\}$.

To sample the particles from their local distributions, we use Stein Variational Gradient Decent (SVGD) [39] which is a particle-based inference approach using a functional gradient decent to approximate a ground-truth distribution known up to a normalizing factor. The update formula of SVGD consists of two terms with different roles: the first term drives the particles towards the high probability areas of the distribution by following a smoothed gradient direction (i.e., the weighted sum of the gradients of all the points weighted by the kernel function), while the second term acts as a repulsive force that prevents all the particles to collapse together into local modes of the distribution [39]. More specifically, to keep the particles inside their balls, we employ projected SVGD as presented in Algorithm 1. In our experiments, we use a RBF kernel with kernel width σ: $k\left(X, \tilde{X}\right) = \exp\left\{ -\left\|X - \tilde{X}\right\| / \left(2\sigma^2\right) \right\}$.

After obtaining the particles $\tilde{X}^S_{kij}$ and $\tilde{X}^T_{ij}$, we make use of them to minimize the objective function in equation (10) for updating $\psi = (\phi, \theta)$. Specifically, we utilize cross-entropy for the classification loss term ℓ and the symmetric Kullback-Leibler (KL) divergence for the local regularization term $s\left(X, \tilde{X}; \psi\right)$ as

$$\frac{1}{2} KL\left(f_\psi\left(X\right) \| f_\psi\left(\tilde{X}\right)\right) + \frac{1}{2} KL\left(f_\psi\left(\tilde{X}\right) \| f_\psi\left(X\right)\right).$$

Finally, the global-regularization function of interest $r^g\left(\left[X^S_{ki}\right]_{k,i}, \left[X^T_i\right]_i; \psi\right)$ is defined accordingly depending on the task and explicitly presented in the sequel.

Algorithm 1 Projected SVGD.

Input: A local distribution around X with an unnormalized density function $\tilde{p}(\cdot)$ and a set of initial particles $\{X^0_i\}^n_{i=1}$.
Output: A set of particles $\{X_i\}^n_{i=1}$ that approximates the local distribution corresponding to $\tilde{p}(\cdot)$.
for $l = 1$ to L **do**
$\quad X^{l+1}_i = \prod_{B_\epsilon(X)}\left[X^l_i + \eta_l \hat{\phi}^*(X^l_i)\right]$
$\quad$ where $\hat{\phi}^*(X) = \frac{1}{n} \sum^n_{j=1}[k(X^l_j, X)\nabla_{X^l_j} \log \tilde{p}(X^l_j) + \nabla_{X^l_j} k(X^l_j, X)]$ and η_l is the step size at
$\quad$ the lth iteration.
end for

3.3 Setting for Domain Adaptation and Semi-supervised Learning

By considering the single source domain as the labeled portion and the target domain as the unlabeled portion, the same setting can be employed for DA and SSL. Particularly, we denote the data/label distribution of the source domain or labeled portion by $\mathbb{P}^{S|l}_1$ and the data distribution of target domain or unlabeled portion by $\mathbb{P}^{T|u}$. Notice that for SSL, $\mathbb{P}^{T|u}$ could be the marginal of $\mathbb{P}^{S|l}$ by marginalizing out the label dimension. Evidently, with this consideration, DA and SSL are special cases of our general framework in Section 3.1, where the global-regularization function of interest $r^g\left(\left[X^S_i\right]_i, \left[X^T_j\right]_j; \psi\right)$ is defined as

$$\mathcal{W}_d\left(\frac{1}{B^S} \sum^{B^S}_{i=1} \delta_{U^S_i}, \frac{1}{B^T} \sum^{B^T}_{j=1} \delta_{U^T_j}\right), \tag{12}$$

where $U^S_i = \left[g_\phi\left(X^S_i\right), h_\theta\left(g_\phi\left(X^S_i\right)\right)\right]$, $U^T_j = \left[g_\phi\left(X^T_j\right), h_\theta\left(g_\phi\left(X^T_j\right)\right)\right]$, and δ is the Dirac delta distribution. The cost metric d is defined as

$$d\left(U^S_i, U^T_j\right) := \rho_d\left(g_\phi\left(X^S_i\right), g_\phi\left(X^T_j\right)\right) + \gamma \rho_l\left(h_\theta\left(g_\phi\left(X^S_i\right)\right), h_\theta\left(g_\phi\left(X^T_j\right)\right)\right)$$

where ρ_d is a metric on the latent space and $\gamma > 0$.

With the global term in equation (12), we aim to reduce the discrepancy gap between the *source (labeled)* domain and the *target (unlabeled)* domain for learning domain-invariant

representations. It is worth noting that this global term in equation (12) was inspected in DeepJDOT [10] for DA setting. Our approach is different from that approach in the local regularization term.

3.4 Setting for Domain Generalization

By setting $B^T = 0$ (i.e., do not use any target data in training), our general framework in Section 3.1 is applicable to DG, where the global-regularization function of interest $r^g \left(\left[X_{ki}^S \right]_{k,i}, \left[X_i^T \right]_i ; \psi \right)$ is defined as

$$\sum_{m=1}^{M} \sum_{k=1}^{K} \frac{1}{K} \mathcal{W}_d \left(\tilde{\mathbb{P}}_{km}, \tilde{\mathbb{P}}_m \right), \tag{13}$$

where the cost metric $d = \rho_d$ is a metric on the latent space, $\tilde{\mathbb{P}}_{km}$ is the empirical distribution over $g_\phi \left(X_{ki}^S \right)$ with $Y_{ki}^S = m$, and $\tilde{\mathbb{P}}_m = \frac{1}{K} \sum_{k=1}^{K} \tilde{\mathbb{P}}_{km}$.

3.5 Setting for Adversarial Machine Learning

For AML, we have only *single source domain* and need to train a deep model which is robust to adversarial examples. We denote the data/label distribution of the source domain by $\mathbb{P}_1^S$ and propose using a dynamic and pseudo target domain of the *on-the-fly adversarial examples* $\left[\left[X_{1ij}^S \right]_{i=1}^{B^S} \right]_{j=1}^{n^S}$. In addition to the local and loss terms as in equation (10), to strengthen model robustness, we propose the following global term to move adversarial examples ($\sim \mathbb{P}^T$) to benign examples ($\sim \mathbb{P}_1^S$):

$$\mathcal{W}_d \left(\frac{1}{B_1^S} \sum_{i=1}^{B_1^S} \delta_{U_i^S}, \frac{1}{B_1^S n^S} \sum_{i=1}^{B_1^S} \sum_{j=1}^{n^S} \delta_{U_{ij}^S} \right), \tag{14}$$

where $U_i^S = \left[g_\phi \left(X_{1i}^S \right), h_\theta \left(g_\phi \left(X_{1i}^S \right) \right) \right]$, $U_{ij}^S = \left[g_\phi \left(X_{1ij}^S \right), h_\theta \left(g_\phi \left(X_{1ij}^S \right) \right) \right]$, and the cost metric d is defined as

$$d \left(U_i^S, U_{ij}^S \right) := \mathbb{I}_{Y_{1i}^S = Y_{1\bar{i}}^S} \left[\rho_d \left(g_\phi \left(X_{1i}^S \right), g_\phi \left(X_{1\bar{i}j}^S \right) \right) + \gamma \rho_l \left(h_\theta \left(g_\phi \left(X_{1i}^S \right) \right), h_\theta \left(g_\phi \left(X_{1\bar{i}j}^S \right) \right) \right) \right], \tag{15}$$

where $\mathbb{I}$ is the indicator function. Here we note that $X_{1\bar{i}j}^S$ is an adversarial example of $X_{1\bar{i}}^S$ which has the ground-truth label $Y_{1\bar{i}}^S$, hence by using the cost metric as in equation (15), we encourage the adversarial example $X_{1\bar{i}j}^S$ to move to a group of the benign examples with the same label.

Finally, to tackle the WS-related terms in equations (12), (13), and (14), we employ the entropic regularization dual form of WS, which had been demonstrated to have favorable computational complexities [37, 38, 36].

Table 1: Single domain generalization accuracy (%) on CIFAR-10-C and CIFAR-100-C datasets with different backbone architectures. We use the **bold** font to highlight the best results.

Datasets	Backbone	Standard	Cutout	CutMix	AutoDA	Mixup	AdvTrain	ADA	ME-ADA	GLOT-DR
	AllConvNet	69.2	67.1	68.7	70.8	75.4	71.9	73	78.2	**82.5**
	DenseNet	69.3	67.9	66.5	73.4	75.4	72.4	69.8	76.9	**83.6**
CIFAR-10-C	WideResNet	73.1	73.2	72.9	76.1	77.7	73.8	79.7	83.3	**84.4**
	ResNeXt	72.5	71.1	70.5	75.8	77.4	73	78	83.4	**84.5**
	Average	71	69.8	69.7	74	76.5	72.8	75.1	80.5	**83.7**
	AllConvNet	43.6	43.2	44	44.9	46.6	44	45.3	51.2	**54.8**
	DenseNet	40.7	40.4	40.8	46.1	44.6	44.8	45.2	47.8	**53.2**
CIFAR-100-C	WideResNet	46.7	46.5	47.1	50.4	49.6	44.9	50.4	52.8	**56.5**
	ResNeXt	46.6	45.4	45.9	48.7	48.6	45.6	53.4	57.3	**58.4**
	Average	44.4	43.9	44.5	47.5	47.4	44.8	48.6	52.3	**55.7**

4 Experiments

To demonstrate the effectiveness of our proposed method, we evaluate its performance on various experiment protocols, including domain generalization, domain adaptation, semi-supervised learning and adversarial machine learning. Due to the space limitation, the detailed setup regarding the architectures and hyperparameters are presented in Appendix B. We tried to use the exact configuration of optimizers and hyper-parameters for all experiments and report the original results in prior work, if possible.

4.1 Experiments for DG

In DG experiments, our setup closely follows [75]. In particular, we validate our method on the CIFAR-C single domain generalization benchmark: train the model on either CIFAR-10 or CIFAR-100 dataset [26], then evaluate it on CIFAR-10-C or CIFAR-100-C [23], correspondingly. In terms of network architectures, we use the exact backbones from [75] to examine the versatility of our method that can be adopt in any type of classifier. GLOT-DR is compared with other state-of-the-art methods in image corruption robustness: Mixup [72], Cutout [12] and Cutmix [70], AutoDA [9], ADA [65], and ME-ADA [75]. Table. 1 shows the average accuracy when we alternatively train the model on one category and evaluate on the rest. In every setting, GLOT-DR outperforms other methods by large margins. Specifically, our method exceeding the second-best method ME-ADA [75] by 3.2% on CIFAR-10-C and 3.4% on CIFAR-100-C. The substantial gain in terms of the accuracy on various backbone architectures demonstrates the high applicability of the proposed techniques.

Furthermore, we examine multi-source DG where the classifier needs to generalize from multiple source domains to an unseen target domain, using the popular PACS dataset [32]. Our proposed method is applicable in this scenario since it is designed to better learn domain invariant features as well as leverage the diversity from generated data. We compare GLOT-DR against DSN [5], L-CNN [32], MLDG [33], Fusion [47], MetaReg [1] and Epi-FCR, AGG [34], HEX [67], and PAR [66]. Table 2 shows that our GLOT-DR outperforms the baselines for three cases and averagely surpasses the second best baseline by 0.9%. The most noticeable improvement is on the Sketch domain ($\approx 2.4\%$), which is the most challenging - the styles of the images are colorless and far different from the ones from Art Painting, Cartoon or Photos (i.e. larger domain shift).

Table 2: Multi-source domain generalization accuracy (%) on PACS datasets. Each column title indicates the target domain used for evaluation, while the rest are for training.

	DSN	L-CNN	MLDG	Fusion	MetaReg	Epi-FCR	AGG	HEX	PAR	ADA	ME-ADA	GLOT-DR
Art	61.1	62.9	66.2	64.1	69.8	64.7	63.4	66.8	66.9	64.3	**67.1**	66.1
Cartoon	66.5	67.0	66.9	66.8	70.4	**72.3**	66.1	69.7	67.1	69.8	69.9	**72.3**
Photo	83.3	89.5	88.0	90.2	91.1	86.1	88.5	87.9	88.6	85.1	88.6	**90.4**
Sketch	58.6	57.5	59.0	60.1	59.2	65.0	56.6	56.3	62.6	60.4	63.0	**65.4**
Average	67.4	69.2	70.0	70.3	72.6	72	68.7	70.2	71.3	69.9	72.2	**73.5**

Table 3: Accuracy (%) on Office-31 [57] of ResNet50 model [22] in unsupervised domain adaptation methods.

Method	A→W	D→W	W→D	A→D	D→A	W→A	Avg
ResNet	68.4	96.7	99.3	68.9	62.5	60.7	76.1
DAN	80.5	97.1	99.6	78.6	63.6	62.8	80.4
RTN	70.2	96.6	95.5	66.3	54.9	53.1	72.8
DANN	84.5	96.8	99.4	77.5	66.2	64.8	81.6
JAN	82	96.9	99.1	79.7	68.2	67.4	82.2
GTA	89.5	97.9	99.8	87.7	72.8	**71.4**	86.5
CDAN	93.1	98.2	**100**	**89.8**	70.1	68	86.6
DeepJDOT	88.9	98.5	99.6	88.2	**72.1**	70.1	86.2
ETD	92.1	**100**	**100**	88	71	67.8	86.2
GLOT-DR	**96.2**	98.9	**100.0**	90.6	68.7	69.9	**87.4**

4.2   Experiments for DA

In this section, we conduct experiments on the commonly used dataset for real-world unsupervised DA - Office-31 [57], comprising 4,110 images in 31 classes from three domains: Amazon (A), Webcam (W) and DSLR (D). Our proposed GLOT-DR is compared against baselines: ResNet-50 [22], DAN [40], RTN [42], DANN [17], JAN [43], GTA [59], CDAN [41], DeepJDOT [10] and ETD [35]. For a fair comparison, we follow the training setups of CDAN and compare with other works using this configuration. As can be seen from Table 3, GLOT-DR achieves the best overall performance among baselines with 87.4% accuracy. Compared with ETD, which is another OT-based domain adaptation method, our performance significantly increase by 4.1% on A→W task, 2.1% on W→A and 1.2% on average.

We further extensively investigate the role of different components in GLOT-DR. Specifically, elimination of the global-regularization term in equation (12) downgrades our method to Local Optimal Transport based Distributional Robustness (LOT-DR). Similarly, when discarding the local distribution robustness term, the attained method is denoted by GOT-DR. We then compare these 2 variants of GLOT-DR to the well-known adversarial machine learning method VAT [48]. To be more specific, in the adversarial samples generation, we apply VAT by perturbing on the: (i) input space, (ii) latent space. Figure 2 shows that the employment of VAT on latent space (orange) is more effective than on the input space (purple), 83% and 80.6%. However, using GOT-DR or LOT-DR is even more effective: performance is boosted to 84.3% and 85.4%, respectively. Lastly, using the full method GLOT-DR yields the highest average accuracy score.
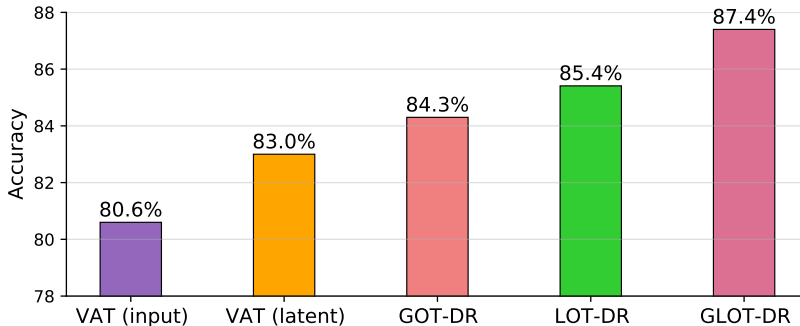
Figure 2: Average accuracy of ResNet50 [22] on Office-31: Comparision between GLOT-DR's variants and VAT [48] on the input and latent spaces . Best viewed in color.
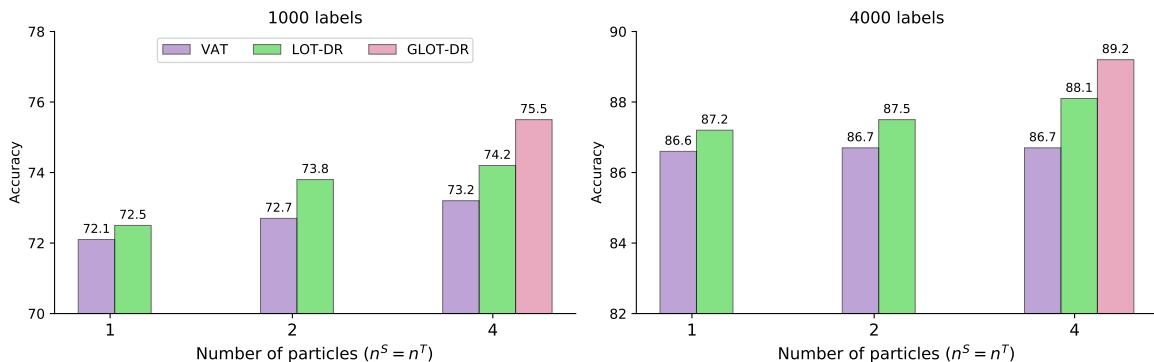

Figure 3: Accuracy (%) on CIFAR-10 of ConvLarge model in SSL settings when using 1,000 and 4,000 labeled examples (i.e. 100 and 400 labeled samples each class, respectively). Best viewed in color.

4.3 Experiments for SSL

Sharing a similar objective with DA, which utilizes the unlabeled samples for improving the model performance, SSL methods can also benefit from our proposed technique. In this section, we present the empirical results on CIFAR-10 benchmark with ConvLarge architecture, following VAT's protocol [48], which serves as a strong baseline in this experiment. We refer readers to Appendix B for more details on the architecture of ConvLarge. Results in Figure 3 (when training with 1000 and 4000 labeled examples) demonstrate that, with only $n^S = n^T = 1$ perturbed sample per anchor, the performance of LOT-DR slightly outperforms VAT with $\sim 0.5\%$. With more perturbed samples per anchor, this gap increases: approximately 1% when $n^S = n^T = 2$ and 1.5% when $n^S = n^T = 4$. Similar to the previous DA experiment, adding the global regularization term helps increase accuracy by approximately 1% in this situation.

4.4 Experiments for AML

Table. 4 shows the evaluation against adversarial examples. We compare our method with PGD-AT [46] and TRADES [74], which are two well-known defense methods in AML. For the sake of fair comparison, we use the same adversarial training setting for all methods which is carefully investigated in [55]. The detail setting can be found in Appendix B. We also compare

Table 4: Adversarial robustness evaluation on CIFAR10 of ResNet18 model. PGD, AA and B&B represent the robust accuracy against the PGD attack (with 10/200 iterations) [46], Auto-Attack [8] and B&B attack [6], respectively, while NAT denotes the natural accuracy.

Method	NAT	PGD10	PGD200	AA	B&B
PGD-AT[*]	82.52	53.58	-	48.51	-
TRADES[*]	81.45	53.51	-	49.06	-
PGD-AT[◇]	83.36	53.52	52.21	49.00	48.50
TRADES[◇]	81.64	53.73	53.11	49.77	49.02
ADT-EXP	83.02	-	45.80	45.80	46.50
ADT-EXPAM	84.11	-	46.10	44.50	45.83
GLOT-DR	**84.13**	**54.13**	**53.1**8	**49.94**	**49.40**

with adversarial distributional training methods [13] (ADT-EXP and ADT-EXPAM), which assume that the adversarial distribution explicitly follows normal distribution. It can be seen from Table 4 that our GLOT-DR method outperforms all these baselines in both natural and robustness performance. Specifically, comparing to PGD-AT, our method has an improvement of 0.8% in natural accuracy and around 1% robust accuracies against PGD200 and AA attacks. Comparing to TRADES, while achieving the same level of robustness, our method has a better performance with benign examples with a gap of 2.5%. Especially, our method significantly outperforms ADT by around 7% under the PGD200 attack.

5 Conclusion

Deep neural networks are vulnerable to adversarial examples and distribution shifts. Although DR is a promising framework to improve model robustness and generalization capability, its current formulation shows some limitations, circumventing its application to real-world problems. First, its formulation is not sufficiently rich to express global regularization term targeting real-world applications. Second, the dual form is not readily trainable to incorporate to deep learning models. In this work, we propose a rich OT based DR framework, named **G**lobal-**L**ocal **O**ptimal **T**ransport based **D**istributional **R**obustness (GLOT-DR) which is sufficiently rich for many real-world applications including DG, DA, SSL, and AML and has a closed-form solution. We conduct comprehensive experiments to compare our GLOT-DR with state-of-the-art baselines accordingly. Empirical results have demonstrated the merits of our GLOT-DR.

---

[*] Results are taken from Pang et al. [55]

[◇] Our reproduced results

Supplement to "Global-Local Regularization Via Distributional Robustness"

This appendix provides proofs of our theory development and additional experiments. This consists of the following sections.

- Appendix A contains the proofs of our theory development.

- Appendix B contains the network architectures, experiment settings of our experiments and additional ablation studies.

A   Proofs of Our Theory Development

We here give the proof for the equivalence in optimizing two equations (6) and (7) in Section A.1. Then, we detail how to derive the optimization formulations (2) and (10) for solving the problems discussed in Section 3.1.

A.1   Proof of Lemma 1

Let

$$\gamma^* = \operatorname*{argmax}_{\gamma: \in \Gamma_\epsilon} \mathbb{E}_{(Z,\tilde{Z}) \sim \gamma}\left[r\left(\tilde{Z}; \phi, \theta\right)\right]$$

be the optimal solution of the inner max in equation (7). Denote $\tilde{\mathbb{P}}^*$ as the distribution obtained from γ^* by maginalizing the dimensions of Z. We prove that $\tilde{\mathbb{P}}^*$ is the optimal solution of the inner max in equation (6). Let $\tilde{\mathbb{P}}$ be a feasible solution of the inner max in equation (6), meaning that $\mathcal{W}_\rho\left(\mathbb{P}, \tilde{\mathbb{P}}\right) \leq \epsilon$. Therefore, there exists $\gamma \in \Gamma\left(\mathbb{P}, \tilde{\mathbb{P}}\right)$ such that $\mathbb{E}_{(Z,\tilde{Z}) \sim \gamma}\left[\rho\left(Z, \tilde{Z}\right)\right]^{1/q} \leq \epsilon$ or $\gamma \in \Gamma_\epsilon$. We have

$$\mathbb{E}_{\tilde{\mathbb{P}}}\left[r\left(\tilde{Z}; \phi, \theta\right)\right] = \mathbb{E}_\gamma\left[r\left(\tilde{Z}; \phi, \theta\right)\right]$$
$$\leq \mathbb{E}_{\gamma^*}\left[r\left(\tilde{Z}; \phi, \theta\right)\right] = \mathbb{E}_{\mathbb{P}^*}\left[r\left(\tilde{Z}; \phi, \theta\right)\right].$$

We reach the conclusion that $\tilde{\mathbb{P}}^*$ is the optimal solution of the inner max in equation (6). That concludes our proof.

A.2   Proof of Theorem 2

Given $\gamma \in \Gamma_\epsilon$, we first prove that if $\mathbb{E}_{(Z,\tilde{Z}) \sim \gamma}\left[\rho\left(Z, \tilde{Z}\right)\right]$ is finite $\forall q > 1$ then

$$M_\gamma := \lim_{q \to \infty} \mathbb{E}_{(Z,\tilde{Z}) \sim \gamma}\left[\rho\left(Z, \tilde{Z}\right)\right]^{1/q} =$$

$$\sup_{(Z,\tilde{Z}) \in \operatorname{supp}(\gamma)} \max\left\{\max_{k,i,j}\left\|X_{kij}^S - \tilde{X}_{kij}^S\right\|_p, \max_{i,j}\left\|X_{ij}^T - \tilde{X}_{ij}^T\right\|_p\right\}$$

Let denote A_γ as the set of $\left(Z, \tilde{Z}\right) \in \operatorname{supp}(\gamma)$ such that

$$\max\left\{\max_{k,i,j}\left\|X_{kij}^S - \tilde{X}_{kij}^S\right\|_p, \max_{i,j}\left\|X_{ij}^T - \tilde{X}_{ij}^T\right\|_p\right\} = M_\gamma.$$

14

We have

$$\mathbb{E}_{(Z,\tilde{Z})\sim\gamma}\left[\rho\left(Z,\tilde{Z}\right)\right]^{1/q} = \left[\int_{A_\gamma}\rho\left(Z,\tilde{Z}\right)d\gamma\left(Z,\tilde{Z}\right) + \int_{A_\gamma^c}\rho\left(Z,\tilde{Z}\right)d\gamma\left(Z,\tilde{Z}\right)\right]^{1/q}.$$

It is obvious that if $\left(Z,\tilde{Z}\right) \sim \gamma$ then

$$\rho\left(Z,\tilde{Z}\right) := \sum_{i=1}^{B^T}\sum_{j=1}^{n^T}\left\|X_{ij}^T - \tilde{X}_{ij}^T\right\|_p^q + \sum_{k=1}^{K}\sum_{i=1}^{B_k^S}\sum_{j=1}^{n^S}\left\|X_{kij}^S - \tilde{X}_{kij}^S\right\|_p^q.$$

Therefore, for $\left(Z,\tilde{Z}\right) \in A_\gamma^c$, we have

$$\lim_{q\to\infty}\frac{\rho\left(Z,\tilde{Z}\right)}{M_\gamma^q} = 0,$$

while for $\left(Z,\tilde{Z}\right) \in A_\gamma$, we have

$$\lim_{q\to\infty}\frac{\rho\left(Z,\tilde{Z}\right)}{M_\gamma^q} = 1.$$

We derive as

$$\lim_{q\to\infty}\mathbb{E}_{(Z,\tilde{Z})\sim\gamma}\left[\rho\left(Z,\tilde{Z}\right)\right]^{1/q} = M_\gamma\lim_{q\to\infty}\left[\int_{A_\gamma}\frac{\rho\left(Z,\tilde{Z}\right)}{M^q}d\gamma\left(Z,\tilde{Z}\right) + \int_{A_\gamma^c}\frac{\rho\left(Z,\tilde{Z}\right)}{M^q}d\gamma\left(Z,\tilde{Z}\right)\right]^{1/q}$$

$$= M_\gamma\lim_{q\to\infty}\gamma\left(A_\gamma\right)^{1/q} = M_\gamma.$$

Therefore, $\gamma \in \Gamma_\epsilon$ with $q = \infty$ is equivalent to the fact that the support set $\mathrm{supp}\left(\gamma\right)$ is the union of B_Z with $Z \in \mathrm{supp}\left(\mathbb{P}\right)$, where B_Z is defined as follows:

$$B_Z := \prod_{k=1}^{K}\prod_{i=1}^{B_k^S}\prod_{j=0}^{n_k^S}B_\epsilon\left(X_{kij}^S\right)\prod_{i=1}^{B^T}\prod_{j=1}^{n^T}B_\epsilon\left(X_{ij}^T\right)$$

$$= \prod_{k=1}^{K}\prod_{i=1}^{B_k^S}\prod_{j=0}^{n_k^S}B_\epsilon\left(X_{ki}^S\right)\prod_{i=1}^{B^T}\prod_{j=1}^{n^T}B_\epsilon\left(X_i^T\right).$$

We can equivalently turn the optimization problem in equation (8) as follows:

$$\max_{\gamma\in\Gamma}\mathbb{E}_{(Z,\tilde{Z})\sim\gamma}\left[r\left(\tilde{Z};\phi,\theta\right)\right] + \frac{1}{\lambda}\mathbb{H}\left(\gamma\right) \tag{16}$$

$$\text{s.t.} : \mathrm{supp}\left(\gamma\right) = \cup_{Z\in\,\mathrm{supp}(\mathbb{P})}B_Z,$$

where $\Gamma = \cup_{\tilde{\mathbb{P}}}\Gamma\left(\mathbb{P},\tilde{\mathbb{P}}\right)$.

15

Because $\gamma \in \Gamma\left(\mathbb{P}, \tilde{\mathbb{P}}\right)$ for some $\tilde{\mathbb{P}}$, we can parameterize its density function as:

$$\gamma\left(Z, \tilde{Z}\right) = p\left(Z\right) \tilde{p}\left(\tilde{Z} \mid Z\right),$$

where $p\left(Z\right)$ is the density function of $\mathbb{P}$ and $\tilde{p}\left(\tilde{Z} \mid Z\right)$ has the support set B_Z. Please note that the constraint for $\tilde{p}\left(\tilde{Z} \mid Z\right)$ is $\int_{B_Z} \tilde{p}\left(\tilde{Z} \mid Z\right) d\tilde{Z} = 1$.

The Lagrange function for the optimization problem in equation (16) is as follows:

$$\begin{aligned}
\mathcal{L} = &\int r\left(\tilde{Z}; \phi, \theta\right) p\left(Z\right) \tilde{p}\left(\tilde{Z} \mid Z\right) dZ d\tilde{Z} \\
&- \frac{1}{\lambda} \int p\left(Z\right) \tilde{p}\left(\tilde{Z} \mid Z\right) \log\left[p\left(Z\right) \tilde{p}\left(\tilde{Z} \mid Z\right)\right] dZ d\tilde{Z} \\
&+ \int \alpha\left(Z\right)\left[\tilde{p}\left(\tilde{Z} \mid Z\right) d\tilde{Z} - 1\right] d\tilde{Z} dZ,
\end{aligned}$$

where the integral w.r.t Z over on supp $\left(\mathbb{P}\right)$ and the one w.r.t. $\tilde{Z}$ over B_Z.

Taking the derivative of $\mathcal{L}$ w.r.t. $\tilde{p}\left(\tilde{Z} \mid Z\right)$ and setting it to 0, we obtain

$$0 = r\left(\tilde{Z}; \phi, \theta\right) p\left(Z\right) + \alpha\left(Z\right) - \frac{p\left(Z\right)}{\lambda}\left[\log p\left(Z\right) + \log \tilde{p}\left(\tilde{Z} \mid Z\right) + 1\right].$$

$$\tilde{p}\left(\tilde{Z} \mid Z\right) = \frac{\exp\left\{\lambda\left[r\left(\tilde{Z}; \phi, \theta\right) + \frac{\alpha(Z)}{p(Z)}\right] - 1\right\}}{p\left(Z\right)}.$$

Taking into account $\int_{B_Z} \tilde{p}\left(\tilde{Z} \mid Z\right) d\tilde{Z} = 1$, we achieve

$$\int_{B_Z} \exp\left\{\lambda r\left(\tilde{Z}; \phi, \theta\right)\right\} d\tilde{Z} = \frac{p\left(Z\right)}{\exp\left\{\lambda \frac{\alpha(Z)}{p(Z)} - 1\right\}}.$$

Therefore, we arrive at

$$\tilde{p}^*\left(\tilde{Z} \mid Z\right) = \frac{\exp\left\{\lambda r\left(\tilde{Z}; \phi, \theta\right)\right\}}{\int_{B_Z} \exp\left\{\lambda r\left(\tilde{Z}; \phi, \theta\right)\right\} d\tilde{Z}}.$$

$$\gamma^*\left(Z, \tilde{Z}\right) = p\left(Z\right) \frac{\exp\left\{\lambda r\left(\tilde{Z}; \phi, \theta\right)\right\}}{\int_{B_Z} \exp\left\{\lambda r\left(\tilde{Z}; \phi, \theta\right)\right\} d\tilde{Z}}. \tag{17}$$

Finally, by noting that

$$p\left(Z\right) = \prod_{k=1}^{K} \prod_{i=1}^{B_k^S} \prod_{j=0}^{n_k^S} p_k^S\left(X_{ki}^S, Y_{ki}^S\right) \prod_{i=1}^{B^T} \prod_{j=0}^{n^T} p^T\left(X_i^T\right) \exp\left\{\lambda r\left(\tilde{Z}; \phi, \theta\right)\right\}$$

$$= \exp\left\{\lambda\beta r^g\left(\tilde{Z};\psi\right)\right\} \prod_{k=1}^{K}\prod_{i=1}^{B_k^S}\prod_{j=0}^{n_k^S} \exp\left\{\lambda[\alpha s(X_{ki}^S, \tilde{X}_{kij}^S;\psi) + \ell(\tilde{X}_{kij}^S, Y_{ki}^S;\psi)]\right\}$$

$$\prod_{i=1}^{B^T}\prod_{j=1}^{n^T} \exp\left\{\lambda\alpha s\left(X_i^T, \tilde{X}_{ij}^T;\psi\right)\right\}.$$

And

$$\int_{B_Z} \exp\left\{\lambda r\left(\tilde{Z};\phi,\theta\right)\right\} d\tilde{Z} = \exp\left\{\lambda\beta r^g\left(\tilde{Z};\psi\right)\right\}$$

$$\prod_{k=1}^{K}\prod_{i=1}^{B_k^S}\prod_{j=0}^{n_k^S} \int_{B_\epsilon(X_{ki}^S)} \exp\left\{\lambda[\alpha s(X_{ki}^S, \tilde{X}_{kij}^S;\psi) + \ell(\tilde{X}_{kij}^S, Y_{ki}^S;\psi)]\right\} d\tilde{X}_{kij}^S$$

$$\prod_{i=1}^{B^T}\prod_{j=1}^{n^T} \int_{B_\epsilon(X_i^T)} \exp\left\{\lambda\alpha s\left(X_i^T, \tilde{X}_{ij}^T;\psi\right)\right\} d\tilde{X}_{ij}^T,$$

we reach the conclusion.

A.3   Proof of the optimization problem in equation (10)

By substituting $\gamma^*\left(Z, \tilde{Z}\right)$ in equation (17) back to the objective function in (7), we obtain

$$\min_\psi \min_{\theta,\phi} \max_{\gamma:\in\Gamma_\epsilon} \mathbb{E}_{(Z,\tilde{Z})\sim\gamma^*}\left[r\left(\tilde{Z};\phi,\theta\right)\right].$$

By referring to the construction of Z and $\tilde{Z}$ and noting that for $\left(Z, \tilde{Z}\right)\sim\gamma^*$

$$r^l\left(\tilde{Z};\psi\right) := \sum_{i=1}^{B^T}\sum_{j=1}^{n^T} s\left(\tilde{X}_{i0}^T, \tilde{X}_{ij}^T;\psi\right) + \sum_{k=1}^{K}\sum_{i=1}^{B_k^S}\sum_{j=1}^{n_k^S} s\left(\tilde{X}_{ki0}^S, \tilde{X}_{kij}^S;\psi\right)$$

$$= \sum_{i=1}^{B^T}\sum_{j=1}^{n^T} s\left(X_i^T, \tilde{X}_{ij}^T;\psi\right) + \sum_{k=1}^{K}\sum_{i=1}^{B_k^S}\sum_{j=1}^{n_k^S} s\left(X_{ki}^S, \tilde{X}_{kij}^S;\psi\right)$$

$$\mathcal{L}\left(\tilde{Z};\psi\right) := \sum_{k=1}^{K}\sum_{i=1}^{B_k^S}\sum_{j=0}^{n_k^S} \ell\left(\tilde{X}_{kij}^S, Y_{ki}^S;\psi\right),$$

we gain the final optimization problem.

B   Implementation Details

In this section, we provide the detailed implementation for all of our experiments along with some additional experimental results.

B.1 Entropic Regularized Duality for WS

To enable the application of optimal transport in machine learning and deep learning, Genevay et al. developed an entropic regularized dual form in [20]. First, they proposed to add an entropic regularization term to the primal form:

$$\mathcal{W}_d^\epsilon\left(\mathbb{P},\mathbb{Q}\right) := \min_{\gamma\in\Gamma(\mathbb{Q},\mathbb{P})}\left\{\mathbb{E}_{(\mathbf{x},\mathbf{y})\sim\gamma}\left[d\left(\mathbf{x},\mathbf{y}\right)\right] + \epsilon D_{KL}\left(\gamma\|\mathbb{P}\otimes\mathbb{Q}\right)\right\}$$

where ϵ is the regularization rate, $D_{KL}\left(\cdot\|\cdot\right)$ is the Kullback-Leibler (KL) divergence, and $\mathbb{P}\otimes\mathbb{Q}$ represents the specific coupling in which $\mathbb{Q}$ and $\mathbb{P}$ are independent. Note that when $\epsilon\to 0$, $\mathcal{W}_d^\epsilon\left(\mathbb{P},\mathbb{Q}\right)$ approaches $\mathcal{W}_d\left(\mathbb{P},\mathbb{Q}\right)$ and the optimal transport plan γ_ϵ^* of equation (18) also weakly converges to the optimal transport plan γ^* of the primal form. In practice, we set ϵ to be a small positive number, hence γ_ϵ^* is very close to γ^*. Second, using the Fenchel-Rockafellar theorem, they obtained the following dual form w.r.t. the potential ϕ

$$\mathcal{W}_d^\epsilon\left(\mathbb{P},\mathbb{Q}\right) = \max_\phi\left\{\int\phi_\epsilon^c\left(\mathbf{x}\right)\mathrm{d}\mathbb{Q}\left(\mathbf{x}\right) + \int\phi\left(\mathbf{y}\right)\mathrm{d}\mathbb{P}\left(\mathbf{y}\right)\right\}$$
$$= \max_\phi\left\{\mathbb{E}_\mathbb{Q}\left[\phi_\epsilon^c\left(\mathbf{x}\right)\right] + \mathbb{E}_\mathbb{P}\left[\phi\left(\mathbf{y}\right)\right]\right\}, \tag{18}$$

where $\phi_\epsilon^c\left(\mathbf{x}\right) := -\epsilon\log\left(\mathbb{E}_\mathbb{P}\left[\exp\left\{\frac{-d(\mathbf{x},\mathbf{y})+\phi(\mathbf{y})}{\epsilon}\right\}\right]\right)$.

In order to calculate the global WS-related regularization terms in equations (12), (13), and (14), we apply the above entropic regularized dual form. The Kantorovich potential network ϕ is a simple network with two fully connected layers with ReLU activation in the middle: $\mathrm{FC}_{\text{latent\_dim}\times 512}\to\mathrm{ReLU}\to\mathrm{FC}_{512\times 1}$ is used throughout experiments. Note that the latent_dim depends on the main network.

Additionally, the distance ρ_d in equation (13) used in all experiments is the Euclidean distance $\mathrm{d}(\mathrm{x}_1,\mathrm{x}_2) = ||\mathrm{x}_1-\mathrm{x}_2||_2^2$, the prediction discrepancy trade-off γ is set equal to 0.5, and the entropic regularization parameter λ in equation (8) is 0.1.

B.2 Projected SVGD Setting

For Projected SVGD in Algorithm 1, we employ an RBF kernel

$$k\left(X,\tilde{X}\right) = \exp\left\{\frac{-\left\|X-\tilde{X}\right\|_2^2}{2\sigma^2}\right\},$$

where the kernel width is set according to the main paper [39].

B.3 Experiments for DG

B.3.1 Network Architecture and Hyperparamters

As mentioned in the main paper, we incorporate well-studied backbones for our experiments, following the implementation of for single domain generalization tasks in [75]. In particular:

Table 5: Details on the domain generalization benchmark datasets

Dataset	# classes	Shape
MNIST [30]	10	32×32
SVHN [54]	10	32×32
MNIST-M [16]	10	32×32
SYN [16]	10	32×32
USPS [11]	10	32×32
CIFAR-10-C [23]	15	$3 \times 32 \times 32$
CIFAR-100-C [23]	15	$3 \times 32 \times 32$
PACS [32]	7	$3 \times 224 \times 224$

- LeNet5 [29] is employed in the MNIST experiment. We first pre-train the network on the MNIST dataset without applying any DG method for 100 iterations, then on each iteration 100, 200, 300 we generate particles with $n^S = n^T = n \in \{1, 2, 4\}$ by running the Projected SVGD sampling1 in $L = 15$ iterations, step size $\eta = 0.002$. We use Adam optimizer [25] with learning rate 10^{-5} and train for 15000 iteration in total with batch size of 32.

- CIFAR-C [1] experiment uses 4 different backbone architectures, namely: All Convolutional Network (AllConvNet) [62], DenseNet [24] , WideResNet [71], and ResNeXt [69]. We set $n^S = n^T = n = 2$ particles, $L = 15$ iterations, step size $\eta = 0.001$ and minimize the loss with SGD optimizer with initial learning rate of 0.1 and batch size 128. Similar to MNIST experiment, we first pretrain the network for 10 epochs then generate augmented images on epoch 10 and 20, number of total epochs required for training are 150 in the case of AllConvNet and WideResNet, 250 epochs for DenseNet and ResNeXt.

- We used an AlexNet [27] pretrained on ImageNet [56] in the PACS experiment. Different from the two above experiments, which generate augmented images and append them directly to the training set, we generate the augmented images in each mini-batch and calculate the local/global regularization terms. $n^S = n^T$ are set qual to 2, $L = 15$ iterations, step size $\eta = 0.007$. The initial global and local trade-off are 3.10^{-5} and 50, these parameters are is adjusted by $\frac{iter}{\#num\_iter}$ in iter-th iteration. We train AlexNet for 45.000 iterations with SGD optimizer and 10^{-3} learning rate.

B.3.2 Datasets and Baselines

We present the details on each dataset used in domain generalization experiments in Table. 5. Digits datasets: MNIST [30], SVHN [54], MNIST-M [16], SYN [16], USPS [11] - each contains 10 classes from $0 - 9$, which are resized to 32×32 images in our experiment. CIFAR-10-C [23], and CIFAR-100-C [23] consist of corrupted images from the original CIFAR [26] datasets with 15 corruptions types applied. In terms of multi-source domain generalization, we test our proposed model on PACS dataset [32], which includes $3 \times 224 \times 224$ images from four different datasets, including Photo, Art painting, Cartoon, and Sketch.

---

[1]Note that in both CIFAR-C and MNIST experiments, we are provided with only a single source domain, thus GLOT-DR downgrades exactly to LOT-DR.

Table 6: Average classification accuracy (%) on MNIST benchmark, we first train the LeNet5 [29] architecture on MNIST then evaluate on SVHN, MNIST-M, SYN, USPS. We repeat experiment for 10 times and report the mean value and standard deviation.

	SVHN	MNIST-M	SYN	USPS	Average
Standard (ERM)	31.95± 1.91	55.96± 1.39	43.85± 1.27	79.92± 0.98	52.92± 0.98
PAR	36.08± 1.27	61.16 ± 0.21	45.48± 0.35	79.95± 1.18	55.67 ± 0.33
ADA	35.70 ± 2.00	58.65± 1.72	47.18± 0.61	80.40± 1.70	55.48± 0.74
ME-ADA	42.00± 1.74	63.98± 1.82	49.80± 1.74	79.10± 1.03	58.72± 1.12
GLOT-DR n=1	42.70 ± 1.03	67.72 ± 0.63	**50.53 ± 0.88**	82.32 ± 0.63	60.82 ± 0.79
GLOT-DR n=2	42.35 ± 1.44	67.95 ± 0.56	**50.53 ± 0.99**	82.33 ± 0.61	60.81± 0.90
GLOT-DR n=4	**43.10 ± 1.16**	**68.44 ± 0.46**	50.49 ± 1.04	**82.48 ± 0.51**	**61.13 ± 0.79**

In the digits experiment, 10000 images are sellected from MNIST dataset as the training set for the source domain and the other four data sets as the target domains: SVHN , MNIST-M, SYN , USPS. We compare our method with the following baselines: (i) Empirical Risk Minimization (ERM), (ii) PAR [66], (iii) ADA [65] and (iv) ME-ADA [75]. For a fair comparison, we did not use any data augmentation in this digits experiment, all the samples are considered as RGB images (we duplicate the channels if they are grayscale images).

B.3.3 Experimental Results

Table. 6 shows that our model achieves the highest average accuracy compared to the other baselines for all values of $n^S = n^T = n \in \{1, 2, 4\}$, with the highest overall score when $n = 4$. In particular, we observe the highest improvement in MNIST-M target domain of $\approx 5\%$, and $\approx 2.5\%$ overall. Our GLOT-DR also exhibits more consistent with smaller variation in terms of accuracy between runs compared to the second-best method, $(0.79\% - 1.12\%)$.

B.4 Experiments for DA

B.4.1 Network architectures and Hyperparameters

The ResNet50 [22] architecture pretrained on ImageNet, followed by a two fully connected layers classifier. is the same as that of the previous work. We evaluate GLOT-DR on the standard object image classification benchmarks in domain adaptation: Office-31 and ImageCLEF-DA. The proposed method is employed on the latent space, trade-off parameters for global and local terms are set equal to 0.02 and 5 throughout all the DA experiments. We train the ResNet50 model for 10000 steps with batch size of 36, following the standard protocols in [41], with data augmentation techniques like random flipping and cropping.

B.4.2 Dataset

The details of the Office-31 [57] dataset is provided in the main paper, we conduct one more experiment on another dataset: ImageCLEF-DA, containing 12 categories from three public datasets: Caltech-256 (C), ImageNet ILSVRC 2012 (I) and Pascal VOC 2012 (P). Each of these domains includes 50 images per class and 600 in total, which were resized to $3 \times 224 \times 224$ in our experiment. We evaluate all baselines in 6 adaptation scenarios.

Table 7: Accuracy (%) on ImageCLEF-DA of ResNet50 model [22] in unsupervised domain adaptation methods. We set the number of particles $n_S = n_T = 4$ for the local regularization.

	I→P	P→I	I→C	C→I	C→P	P→C	Avg
ResNet	74,8	83,9	91,5	78,0	65,5	91,3	80,7
DAN	74,8	83,9	91,5	78,0	65,5	91,3	80,7
DANN	75,0	86,0	96,2	87,0	74,3	91,5	85,0
JAN	76,8	88,4	94,8	89,5	74,2	91,7	85,8
CDAN	76,7	90,6	97,0	90,5	74,5	93,5	87,1
ETD	**81,0**	91,7	**97,9**	**93,3**	79,5	95,0	89,7
GLOT-DR	79.8	**93.7**	**97.9**	**93.3**	**79.7**	**96.0**	**90.1**
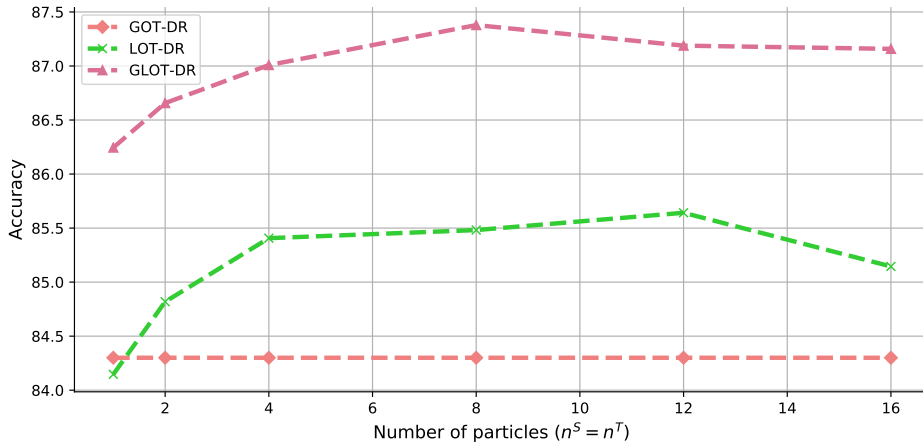
Figure 4: Classification accuracy when varying the number of generated examples sampled from Project SVGD Algorithm.1.

B.4.3 Experimental Results

As reported in Table. 7, the GLOT-DR approach outperforms the comparison methods on nearly all settings, except the pair of I→P, where our score is 1% below ETD [35]. Our proposed method achieves 90.1% average accuracy overall, which is highest compared to all baselines.

Up till now, we have almost finished the needed experiments to examine the effectiveness of our method on domain adaptation. In this ultimate experiment, we illustrate the strength of our proposed regularization technique by varying the number of generated adversarial examples (i.e. n^S and n^T) from 1 to 16. Results are presented in Figure 4, where we perform extensive experiment via comparing GLOT-DR against its variants on different values of n^S, n^T. It can be easily seen that, increasing the number of generated samples can consistently improves the performance in both LOT-DR and GLOT-DR (note that in GOT-DR there is no local regularization term involved, thus there is no difference between different number of samples). Setting $n^S = n^T \geq 2$ helps LOT-DR surpass the performance of GOT-DR.

21

B.5 Experiments for SSL

B.5.1 Network architectures and Hyperparameters

In the semi supervised learning experiment, our main competitor is Virtual Adversarial Training (VAT) [48], we thus replicate their Conv-Large[2] architecture as:

$$32 \times 32 \, \text{RGB image} \rightarrow 3 \times 3 \, \text{conv.128 LReLU}$$
$$\rightarrow 3 \times 3 \, \text{conv.128 LReLU} \rightarrow 3 \times 3 \, \text{conv.128 LReLU}$$
$$\rightarrow 2 \times 2 \, \text{MaxPool, stride 2} \rightarrow \text{Dropout}(0.5)$$
$$\rightarrow 3 \times 3 \, \text{conv.256 LReLU} \rightarrow 3 \times 3 \, \text{conv.256 LReLU}$$
$$\rightarrow 3 \times 3 \, \text{conv.256 LReLU} \rightarrow 2 \times 2 \, \text{MaxPool, stride 2}$$
$$\rightarrow \text{Dropout}(0.5) \rightarrow 3 \times 3 \, \text{conv.512 LReLU}$$
$$\rightarrow 1 \times 1 \, \text{conv.256 LReLU} \rightarrow 1 \times 1 \, \text{conv.128 LReLU}$$
$$\rightarrow \text{Global Average Pool}, 6 \times 6 \rightarrow 1 \times 1 \rightarrow \text{FC}_{128 \times 10}$$

We train the Conv-Large network in 600 epochs with batch size of 128 using SGD optimizer and cosine annealing learning rate scheduler [44]. The global and local trade-off parameters are ajusted by exponential rampup from [58]:

$$\tau = \begin{cases} \exp^{-5(1 - \frac{\text{epoch}}{\text{rampup length}})^2} & \text{epoch} < \text{rampup length} \\ 1 & \text{otherwise} \end{cases}$$

with rampup length = 30 and initial trade-off for global and local terms are 0.1 and 10, respectively.

B.5.2 Experimental Results

In this section, we compare the training time in section 4.3 of LOT-DR and GLOT-DR against VAT in a single epoch. We repeat this process several times to get the average results, which are plotted in Figure 5. While VAT and LOT-DR run in almost equivalent time for all values of generated examples, GLOT-DR requires approximately 25% extra running time. Note that this is worthy because of the superior performance and great flexibility it brings on different scenarios.

B.6 Experiments for AML

B.6.1 General setting

We follow the setting in [55] for the experiment on adversarial machine learning domain. Specifically, the experiment has been conducted on CIFAR-10 dataset with ResNet18 architecture. All models have been trained with 110 epochs with SGD optimizer with momentum 0.9, weight decay 5×10^{-4}. The initial learning rate is 0.1 and reduce at epoch 100-th and 105-th with rate 0.1 as mentioned in [55].

---

[2]LReLU indicates the Leaky ReLU [45] activation function with the negative slope equal to 0.1.
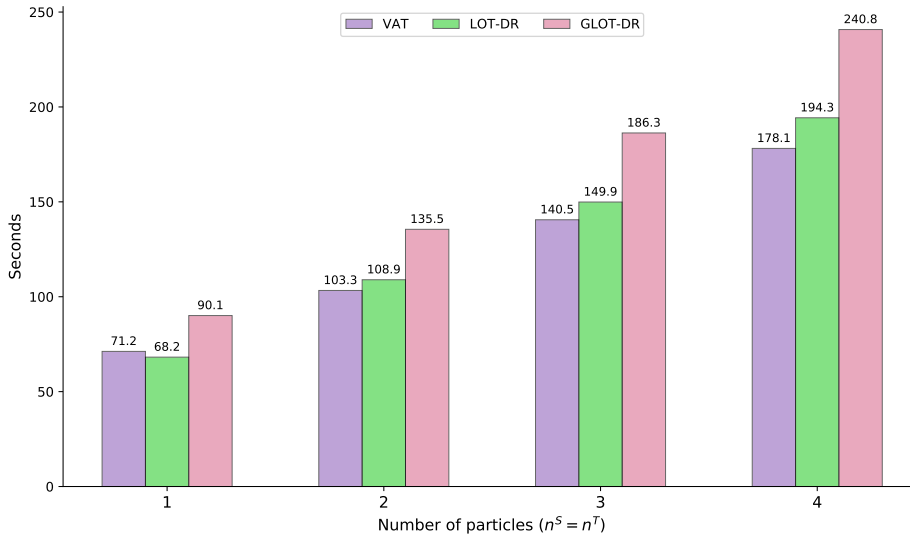
Figure 5: Running time of our proposed approach on: Intel(R) Xeon(R) CPU @ 2.00GHz CPU and Tesla P100 16GB VRAM GPU. Results are averaged over 3 runs.

B.6.2   Attack setting

We use different SOTA attacks to evaluate the defense methods including: (1) PGD attack [46] which is a gradient based attack with parameter $\{k = 200, \epsilon = 8/255, \eta = 2/255\}$ where k is the number of attack iterations, ϵ is the perturbation boundary and η is the step size of each iteration. (2) Auto-Attack (AA) [8] which is an ensemble methods of four different attacks. We use standard version with $\epsilon = 8/255$. (3) B&B attack [6] which is a decision based attack. Following [64], we initialized with the PGD attack with $k = 20, \epsilon = 8/255, \eta = 2/255$ then apply B&B attack with 200 steps. We use L_∞ for measuring the perturbation size and we use the full test set of 10k samples of the CIFAR-10 dataset in all experiments.

B.6.3   Baseline setting

We compare our method with PGD-AT [46] and TRADES [74] which are two well-known defense methods in AML. PGD-AT seeks the most violating examples that maximize the loss w.r.t. the true hard-label $\mathcal{L}_{CE}(h_\theta(x_a), y)$ while TRADES seeks the most divergent examples by maximizing the KL-divergence w.r.t. the current prediction (as consider as a soft-label) $\mathcal{L}_{KL}(h_\theta(x_a) \parallel h_\theta(x))$. To be fair comparison, we use the same training setting for all methods, and succesfully reproduce performance of PGD-AT and TRADES as reported in [55]. We also compare with adversarial distributional training [13] (ADT-EXP and ADT-EXPAM) which assume that the adversarial distribution explicitly follows normal distribution.

23

References

[1] Y. Balaji, S. Sankaranarayanan, and R. Chellappa. Metareg: Towards domain generalization using meta-regularization. *Advances in Neural Information Processing Systems*, 31:998–1008, 2018. (Cited on pages 3 and 10.)

[2] A. Ben-Tal, D. Den Hertog, A. De Waegenaere, B. Melenberg, and G. Rennen. Robust solutions of optimization problems affected by uncertain probabilities. *Management Science*, 59(2):341–357, 2013. (Cited on page 3.)

[3] J. Blanchet, Y. Kang, and K. Murthy. Robust wasserstein profile inference and applications to machine learning. *Journal of Applied Probability*, 56(3):830–857, 2019. (Cited on page 3.)

[4] J. Blanchet and K. Murthy. Quantifying distributional model risk via optimal transport. *Mathematics of Operations Research*, 44(2):565–600, 2019. (Cited on pages 1, 2, and 3.)

[5] K. Bousmalis, G. Trigeorgis, N. Silberman, D. Krishnan, and D. Erhan. Domain separation networks. *Advances in neural information processing systems*, 29:343–351, 2016. (Cited on pages 3 and 10.)

[6] W. Brendel, J. Rauber, M. Kümmerer, I. Ustyuzhaninov, and M. Bethge. Accurate, reliable and fast robustness evaluation. *arXiv preprint arXiv:1907.01003*, 2019. (Cited on pages 13 and 23.)

[7] A. Bui, T. Le, H. Zhao, P. Montague, O. deVel, T. Abraham, and D. Phung. Improving adversarial robustness by enforcing local and global compactness. In *Proceedings of ECCV*, pages 209–223. Springer, 2020. (Cited on page 3.)

[8] F. Croce and M. Hein. Reliable evaluation of adversarial robustness with an ensemble of diverse parameter-free attacks. In *Proceedings of ICML*, 2020. (Cited on pages 3, 13, and 23.)

[9] E. D. Cubuk, B. Zoph, D. Mane, V. Vasudevan, and Q. V. Le. Autoaugment: Learning augmentation strategies from data. In *Proceedings of the IEEE/CVF Conference on Computer Vision and Pattern Recognition*, 2019. (Cited on page 10.)

[10] B. B. Damodaran, B. Kellenberger, R. Flamary, D. Tuia, and N. Courty. Deepjdot: Deep joint distribution optimal transport for unsupervised domain adaptation. In *Proceedings of the European Conference on Computer Vision (ECCV)*, pages 447–463, 2018. (Cited on pages 3, 9, and 11.)

[11] J. S. Denker, W. Gardner, H. P. Graf, D. Henderson, R. E. Howard, W. Hubbard, L. D. Jackel, H. S. Baird, and I. Guyon. Neural network recognizer for hand-written zip code digits. In *Advances in neural information processing systems*, pages 323–331. Citeseer, 1989. (Cited on page 19.)

[12] T. DeVries and G. W. Taylor. Improved regularization of convolutional neural networks with cutout. *arXiv preprint arXiv:1708.04552*, 2017. (Cited on pages 1 and 10.)

[13] Y. Dong, Z. Deng, T. Pang, J. Zhu, and H. Su. Adversarial distributional training for robust deep learning. *Advances in Neural Information Processing Systems*, 33:8270–8283, 2020. (Cited on pages 1, 3, 13, and 23.)

[14] J. C. Duchi, P. W. Glynn, and H. Namkoong. Statistics of robust optimization: A generalized empirical likelihood approach. *Mathematics of Operations Research*, 2021. (Cited on page 3.)

[15] J. C. Duchi, T. Hashimoto, and H. Namkoong. Distributionally robust losses against mixture covariate shifts. *Under review*, 2019. (Cited on page 3.)

[16] Y. Ganin and V. Lempitsky. Unsupervised domain adaptation by backpropagation. In *Proceedings of ICML*, pages 1180–1189. PMLR, 2015. (Cited on page 19.)

[17] Y. Ganin, E. Ustinova, H. Ajakan, P. Germain, H. Larochelle, F. Laviolette, M. Marchand, and V. Lempitsky. Domain-adversarial training of neural networks. *The journal of machine learning research*, 17(1):2096–2030, 2016. (Cited on pages 3 and 11.)

[18] R. Gao, X. Chen, and A. J. Kleywegt. Wasserstein distributional robustness and regularization in statistical learning. *arXiv e-prints*, pages arXiv–1712, 2017. (Cited on page 1.)

[19] R. Gao and A. J. Kleywegt. Distributionally robust stochastic optimization with wasserstein distance. *arXiv preprint arXiv:1604.02199*, 2016. (Cited on page 3.)

[20] A. Genevay, M. Cuturi, G. Peyré, and F. Bach. Stochastic optimization for large-scale optimal transport. In *Advances in Neural Information Processing Systems*, volume 29. Curran Associates, Inc., 2016. (Cited on page 18.)

[21] I. J. Goodfellow, J. Shlens, and C. Szegedy. Explaining and harnessing adversarial examples. *arXiv preprint arXiv:1412.6572*, 2014. (Cited on page 3.)

[22] K. He, X. Zhang, S. Ren, and J. Sun. Deep residual learning for image recognition. In *Proceedings of CVPR*, pages 770–778, 2016. (Cited on pages 11, 12, 20, and 21.)

[23] D. Hendrycks and T. Dietterich. Benchmarking neural network robustness to common corruptions and perturbations. *Proceedings of the International Conference on Learning Representations*, 2019. (Cited on pages 10 and 19.)

[24] G. Huang, Z. Liu, L. Van Der Maaten, and K. Q. Weinberger. Densely connected convolutional networks. In *Proceedings of the IEEE conference on computer vision and pattern recognition*, pages 4700–4708, 2017. (Cited on page 19.)

[25] D. P. Kingma and J. Ba. Adam: A method for stochastic optimization. *Proceedings of the International Conference on Learning Representations*, 2014. (Cited on page 19.)

[26] A. Krizhevsky, G. Hinton, et al. Learning multiple layers of features from tiny images. 2009. (Cited on pages 10 and 19.)

[27] A. Krizhevsky, I. Sutskever, and G. E. Hinton. Imagenet classification with deep convolutional neural networks. *Advances in neural information processing systems*, 25:1097–1105, 2012. (Cited on page 19.)

[28] D. Kuhn, P. M. Esfahani, V. A. Nguyen, and S. Shafieezadeh-Abadeh. Wasserstein distributionally robust optimization: Theory and applications in machine learning. In *Operations Research & Management Science in the Age of Analytics*, pages 130–166. INFORMS, 2019. (Cited on page 3.)

[29] Y. LeCun, B. Boser, J. S. Denker, D. Henderson, R. E. Howard, W. Hubbard, and L. D. Jackel. Backpropagation applied to handwritten zip code recognition. *Neural computation*, 1(4):541–551, 1989. (Cited on pages 19 and 20.)

[30] Y. LeCun, L. Bottou, Y. Bengio, and P. Haffner. Gradient-based learning applied to document recognition. *Proceedings of the IEEE*, 86(11):2278–2324, 1998. (Cited on page 19.)

[31] A. Levine and S. Feizi. Wasserstein smoothing: Certified robustness against wasserstein adversarial attacks. In *International Conference on Artificial Intelligence and Statistics*, pages 3938–3947. PMLR, 2020. (Cited on page 3.)

[32] D. Li, Y. Yang, Y.-Z. Song, and T. M. Hospedales. Deeper, broader and artier domain generalization. In *Proceedings of the IEEE international conference on computer vision*, pages 5542–5550, 2017. (Cited on pages 3, 10, and 19.)

[33] D. Li, Y. Yang, Y.-Z. Song, and T. M. Hospedales. Learning to generalize: Meta-learning for domain generalization. In *Thirty-Second AAAI Conference on Artificial Intelligence*, 2018. (Cited on pages 3 and 10.)

[34] D. Li, J. Zhang, Y. Yang, C. Liu, Y.-Z. Song, and T. M. Hospedales. Episodic training for domain generalization. In *Proceedings of the IEEE/CVF International Conference on Computer Vision*, pages 1446–1455, 2019. (Cited on pages 3 and 10.)

[35] M. Li, Y.-M. Zhai, Y.-W. Luo, P.-F. Ge, and C.-X. Ren. Enhanced transport distance for unsupervised domain adaptation. In *Proceedings of the IEEE/CVF Conference on Computer Vision and Pattern Recognition*, pages 13936–13944, 2020. (Cited on pages 3, 11, and 21.)

[36] T. Lin, N. Ho, X. Chen, M. Cuturi, and M. I. Jordan. Fixed-support Wasserstein barycenters: Computational hardness and fast algorithm. In *NeurIPS*, pages 5368–5380, 2020. (Cited on page 9.)

[37] T. Lin, N. Ho, and M. Jordan. On efficient optimal transport: An analysis of greedy and accelerated mirror descent algorithms. In *ICML*, pages 3982–3991, 2019. (Cited on page 9.)

[38] T. Lin, N. Ho, and M. I. Jordan. On the efficiency of the Sinkhorn and Greenkhorn algorithms and their acceleration for optimal transport. *ArXiv Preprint: 1906.01437*, 2019. (Cited on page 9.)

[39] Q. Liu and D. Wang. Stein variational gradient descent: A general purpose bayesian inference algorithm. In D. Lee, M. Sugiyama, U. Luxburg, I. Guyon, and R. Garnett, editors, *Proceedings of NeurIPS*, volume 29, 2016. (Cited on pages 2, 7, and 18.)

[40] M. Long, Y. Cao, J. Wang, and M. Jordan. Learning transferable features with deep adaptation networks. In F. Bach and D. Blei, editors, *Proceedings of the 32nd International Conference on Machine Learning*, volume 37 of *Proceedings of Machine Learning Research*, pages 97–105, Lille, France, 07–09 Jul 2015. PMLR. (Cited on page 11.)

[41] M. Long, Z. Cao, J. Wang, and M. I. Jordan. Conditional adversarial domain adaptation. *arXiv preprint arXiv:1705.10667*, 2017. (Cited on pages 3, 11, and 20.)

[42] M. Long, H. Zhu, J. Wang, and M. I. Jordan. Unsupervised domain adaptation with residual transfer networks. In D. Lee, M. Sugiyama, U. Luxburg, I. Guyon, and R. Garnett, editors, *Advances in Neural Information Processing Systems*, volume 29. Curran Associates, Inc., 2016. (Cited on page 11.)

[43] M. Long, H. Zhu, J. Wang, and M. I. Jordan. Deep transfer learning with joint adaptation networks. In *International conference on machine learning*, pages 2208–2217. PMLR, 2017. (Cited on page 11.)

[44] I. Loshchilov and F. Hutter. Sgdr: Stochastic gradient descent with warm restarts. *arXiv preprint arXiv:1608.03983*, 2016. (Cited on page 22.)

[45] A. L. Maas, A. Y. Hannun, A. Y. Ng, et al. Rectifier nonlinearities improve neural network acoustic models. In *Proc. icml*, volume 30, page 3. Citeseer, 2013. (Cited on page 22.)

[46] A. Madry, A. Makelov, L. Schmidt, D. Tsipras, and A. Vladu. Towards deep learning models resistant to adversarial attacks. In *International Conference on Learning Representations*, 2018. (Cited on pages 3, 12, 13, and 23.)

[47] M. Mancini, S. R. Bulo, B. Caputo, and E. Ricci. Best sources forward: domain generalization through source-specific nets. In *2018 25th IEEE international conference on image processing (ICIP)*, pages 1353–1357. IEEE, 2018. (Cited on pages 3 and 10.)

[48] T. Miyato, S. Maeda, M. Koyama, and S. Ishii. Virtual adversarial training: A regularization method for supervised and semi-supervised learning. *IEEE Transactions on Pattern Analysis and Machine Intelligence*, 41(8):1979–1993, Aug 2019. (Cited on pages 11, 12, and 22.)

[49] T. Miyato, S.-i. Maeda, M. Koyama, and S. Ishii. Virtual adversarial training: a regularization method for supervised and semi-supervised learning. *IEEE TPAMI*, 41(8):1979–1993, 2018. (Cited on pages 1 and 3.)

[50] T. Miyato, S.-i. Maeda, M. Koyama, K. Nakae, and S. Ishii. Distributional smoothing with virtual adversarial training. *arXiv preprint arXiv:1507.00677*, 2015. (Cited on page 3.)

[51] P. Mohajerin Esfahani and D. Kuhn. Data-driven distributionally robust optimization using the wasserstein metric: Performance guarantees and tractable reformulations. *arXiv e-prints*, pages arXiv–1505, 2015. (Cited on page 3.)

[52] A. Najafi, S.-i. Maeda, M. Koyama, and T. Miyato. Robustness to adversarial perturbations in learning from incomplete data. *Advances in Neural Information Processing Systems*, 32:5541–5551, 2019. (Cited on page 3.)

[53] H. Namkoong and J. C. Duchi. Stochastic gradient methods for distributionally robust optimization with f-divergences. In *NIPS*, volume 29, pages 2208–2216, 2016. (Cited on page 3.)

[54] Y. Netzer, T. Wang, A. Coates, A. Bissacco, B. Wu, and A. Y. Ng. Reading digits in natural images with unsupervised feature learning. In *NIPS Workshop on Deep Learning and Unsupervised Feature Learning 2011*, 2011. (Cited on page 19.)

[55] T. Pang, X. Yang, Y. Dong, H. Su, and J. Zhu. Bag of tricks for adversarial training. In *International Conference on Learning Representations*, 2020. (Cited on pages 12, 13, 22, and 23.)

[56] O. Russakovsky, J. Deng, H. Su, J. Krause, S. Satheesh, S. Ma, Z. Huang, A. Karpathy, A. Khosla, M. Bernstein, et al. Imagenet large scale visual recognition challenge. *International journal of computer vision*, 115(3):211–252, 2015. (Cited on page 19.)

[57] K. Saenko, B. Kulis, M. Fritz, and T. Darrell. Adapting visual category models to new domains. In *European conference on computer vision*, pages 213–226. Springer, 2010. (Cited on pages 11 and 20.)

[58] L. Samuli and A. Timo. Temporal ensembling for semi-supervised learning. In *International Conference on Learning Representations (ICLR)*, volume 4, page 6, 2017. (Cited on page 22.)

[59] S. Sankaranarayanan, Y. Balaji, C. D. Castillo, and R. Chellappa. Generate to adapt: Aligning domains using generative adversarial networks. In *Proceedings of the IEEE Conference on Computer Vision and Pattern Recognition*, pages 8503–8512, 2018. (Cited on page 11.)

[60] S. Shafieezadeh-Abadeh, P. M. Esfahani, and D. Kuhn. Distributionally robust logistic regression. *arXiv preprint arXiv:1509.09259*, 2015. (Cited on page 3.)

[61] A. Sinha, H. Namkoong, and J. Duchi. Certifying some distributional robustness with principled adversarial training. In *International Conference on Learning Representations*, 2018. (Cited on pages 1, 2, and 3.)

[62] J. T. Springenberg, A. Dosovitskiy, T. Brox, and M. Riedmiller. Striving for simplicity: The all convolutional net. *Proceedings of the International Conference on Learning Representations Workshops*, 2014. (Cited on page 19.)

[63] M. Staib and S. Jegelka. Distributionally robust deep learning as a generalization of adversarial training. *NIPS workshop on Machine Learning and Computer Security*, 2017. (Cited on page 3.)

[64] F. Tramer, N. Carlini, W. Brendel, and A. Madry. On adaptive attacks to adversarial example defenses. *Advances in Neural Information Processing Systems*, 33, 2020. (Cited on page 23.)

[65] R. Volpi, H. Namkoong, O. Sener, J. Duchi, V. Murino, and S. Savarese. Generalizing to unseen domains via adversarial data augmentation. *arXiv preprint arXiv:1805.12018*, 2018. (Cited on pages 10 and 20.)

[66] H. Wang, S. Ge, Z. Lipton, and E. P. Xing. Learning robust global representations by penalizing local predictive power. In H. Wallach, H. Larochelle, A. Beygelzimer, F. d'Alché-Buc, E. Fox, and R. Garnett, editors, *Advances in Neural Information Processing Systems*, volume 32. Curran Associates, Inc., 2019. (Cited on pages 10 and 20.)

[67] H. Wang, Z. He, Z. L. Lipton, and E. P. Xing. Learning robust representations by projecting superficial statistics out. In *International Conference on Learning Representations*, 2019. (Cited on page 10.)

[68] H. Wang, A. Liu, Z. Yu, Y. Yue, and A. Anandkumar. Distributionally robust learning for unsupervised domain adaptation, 2021. (Cited on page 3.)

[69] S. Xie, R. Girshick, P. Dollár, Z. Tu, and K. He. Aggregated residual transformations for deep neural networks. In *Proceedings of the IEEE conference on computer vision and pattern recognition*, pages 1492–1500, 2017. (Cited on page 19.)

[70] S. Yun, D. Han, S. J. Oh, S. Chun, J. Choe, and Y. Yoo. Cutmix: Regularization strategy to train strong classifiers with localizable features. In *Proceedings of the IEEE/CVF International Conference on Computer Vision*, pages 6023–6032, 2019. (Cited on pages 1 and 10.)

[71] S. Zagoruyko and N. Komodakis. Wide residual networks. In *Proceedings of the British Machine Vision Conference*, 2016. (Cited on page 19.)

[72] H. Zhang, M. Cisse, Y. N. Dauphin, and D. Lopez-Paz. mixup: Beyond empirical risk minimization. *International Conference on Learning Representations*, 2018. (Cited on pages 1 and 10.)

[73] H. Zhang and J. Wang. Defense against adversarial attacks using feature scattering-based adversarial training. In *Advances in Neural Information Processing Systems*, pages 1829–1839, 2019. (Cited on page 3.)

[74] H. Zhang, Y. Yu, J. Jiao, E. Xing, L. El Ghaoui, and M. Jordan. Theoretically principled trade-off between robustness and accuracy. In *Proceedings of ICML*, pages 7472–7482. PMLR, 2019. (Cited on pages 2, 3, 12, and 23.)

[75] L. Zhao, T. Liu, X. Peng, and D. Metaxas. Maximum-entropy adversarial data augmentation for improved generalization and robustness. In H. Larochelle, M. Ranzato, R. Hadsell, M. F. Balcan, and H. Lin, editors, *Advances in Neural Information Processing Systems*, volume 33, pages 14435–14447. Curran Associates, Inc., 2020. (Cited on pages 1, 3, 10, 18, and 20.)